

FedVSR: Towards Model-Agnostic Federated Learning in Video Super-Resolution

Ali Mollaahmadi Dehaghi¹, Hossein KhademSohi¹, Steve Drew¹, Reza Razavi², Mohammad Moshirpour³

¹ University of Calgary, ² Useful Corporation, ³ University of California, Irvine
{ali.mollaahmadidehag, hossein.khademsohi, steve.drew}@ucalgary.ca,
reza.razavi@useful.com, mmoshirp@uci.edu

Abstract

Video super-resolution aims to enhance low-resolution videos by leveraging both spatial and temporal information. While deep learning has led to impressive progress, it typically requires centralized data, which raises privacy concerns. Federated learning offers a privacy-friendly solution, but general FL frameworks often struggle with low-level vision tasks, resulting in blurry, low-quality outputs. To address this, we introduce FedVSR, the first FL framework specifically designed for VSR. It is model-agnostic and stateless, and introduces a lightweight loss function based on the DWT to better preserve high-frequency details during local training. Additionally, a loss-aware aggregation strategy combines both DWT-based and task-specific losses to guide global updates effectively. Extensive experiments across multiple VSR models and datasets demonstrate that FedVSR consistently outperforms existing FL methods, achieving up to 0.82 dB higher PSNR, 0.0327 higher SSIM, and 0.0251 lower LPIPS. These results underscore FedVSR's ability to bridge the gap between privacy and performance, setting a new benchmark for federated learning in low-level vision tasks. The code is available at: <https://github.com/alimd94/FedVSR>

1. Introduction

Video super-resolution (VSR) is an advanced computational process that reconstructs high-resolution (HR) video sequences from low-resolution (LR) counterparts, leveraging both spatial and temporal information [32]. Unlike single-image super-resolution (SISR), which relies solely on intra-frame details, VSR exploits temporal correlations across consecutive frames to enhance the quality and sharpness of the output. This capability is crucial in real-world applications such as surveillance [12], video streaming [23], and medical imaging [42, 45], where visual fidelity and temporal coherence are mission-critical. In practice, VSR must

also cope with degradations such as down-sampling [60], noise [63], blur [38], and compression artifacts [11]. However, modern deep-learning pipelines address these degradations with data-hungry networks trained on centrally collected data, but centralization itself raises privacy, regulatory, and bandwidth concerns, especially when the raw videos contain sensitive or personally identifiable information.

Federated learning (FL) provides a principled remedy to these concerns [36]. In many VSR scenarios, such as smartphones, surveillance, health-related domains, and remote edge sensors, videos are captured on devices with limited bandwidth and strict privacy constraints. Uploading hours of footage can consume tens of gigabytes of storage; for instance, even a short 10-second 8K video at 30 fps in raw format can exceed 10 GB in size [2]. Additionally, uploading such data may violate policies and laws such as GDPR or HIPAA [19]. Unlike conventional distributed methods that rely on frequent synchronization, FL enables selected participants to perform multiple local updates before their models are aggregated into a global one. This approach minimizes communication overhead and accommodates the limited computational resources of edge devices. These combined benefits make FL a logical and effective foundation for VSR systems that face such concerns.

Despite significant advancements in FL methods, most research has focused on high-level or downstream visual tasks such as image classification [21, 27, 51], facial recognition [34, 41], and segmentation [34, 37]. However, their application in super-resolution (SR) remains largely unexplored. Existing studies [39, 56] found that directly applying existing general FL techniques to SR tasks results in poor-quality reconstructions with blurred textures, mainly due to their inability to effectively capture rich low-level information such as texture, edges and motion. Motivated by these limitations, we propose *FedVSR*, a novel model-agnostic framework for VSR under FL. *FedVSR* treats VSR models as black boxes, allowing it to work with a variety of architectures without requiring architectural changes or



Figure 1. Comparison of RVRT[29] output trained with different federated learning algorithms. General FL methods struggle to reconstruct fine details and textures. PSNR, SSIM, and LPIPS metrics are shown in red, blue, and green respectively.

access to intermediate layers. To improve performance under FL constraints, we introduce a lightweight loss term based on the Discrete Wavelet Transform (DWT), which emphasizes high-frequency details that are often lost during decentralized training. While high-frequency preservation is valuable for all SR tasks, its importance is amplified in VSR due to the added complexity of maintaining temporal coherence across frames. In federated settings, data heterogeneity and limited communication intensify this challenge. *FedVSR* addresses these issues without maintaining state between rounds, making it both scalable and practical for privacy-sensitive, resource-constrained environments. In summary, the main contributions of this paper are as follows:

- We design a frequency-aware loss using DWT to sharpen fine details during client updates, and introduce a complementary aggregation method to weight model contributions more effectively. To the best of our knowledge, this is the first algorithm specifically designed to address VSR in the FL setting, effectively bridging the gap between privacy preservation and reconstruction quality.
- Our approach makes no architecture-specific assumptions and does not require storing past weights, making it stateless and model-agnostic. This design reduces memory usage, avoids privacy risks, and eliminates synchronization overhead in federated learning on edge devices.
- Extensive experiments validate *FedVSR*'s effectiveness, outperforming existing approaches and paving the way for privacy-preserving low-level vision in the FL setting.

2. Related Works

In this section, we begin by discussing the most significant contributions in general FL and VSR. We then explore studies that specifically focus on applying FL to the SR task.

2.1. Federated Learning

Federated learning (FL) is a decentralized learning paradigm that enables multiple clients to collaboratively train models while preserving data privacy. It has been widely applied across diverse domains, including healthcare, finance, and IoT, where data security and regulatory constraints are critical [3, 7, 62]. A foundational approach in this domain is FedAvg [36], which follows a four-step iterative process: (1) the server distributes a global model to all participating clients, (2) each client trains its local model using its own data, (3) the locally updated models are sent back to the central server, and (4) the server aggregates these updates to refine the global model for the next training round.

To enhance the performance of federated learning, multiple methods focus on optimizing local updates. FedProx [27] incorporates a proximal term in the local objective to ensure consistency between local and global models. SCAFFOLD [21] introduces control variates for both clients and the server. FedNova [51] employs normalized averaging to address objective inconsistencies. More recently, MOON [25] applies contrastive learning to assess similarity among different model representations.

2.2. Video Super Resolution

Early VSR methods that applied SISR techniques frame-by-frame neglected the temporal context, resulting in tempo-

ral inconsistencies, loss of detail, and undesired smoothing in the high-resolution output [33]. VSR leverages multiple temporally correlated low-resolution frames within a video sequence to generate high-resolution output. Unlike SISR, VSR must account for both spatial and temporal dependencies across frames, making it a highly complex, non-linear, multi-dimensional problem.

Recent advancements in VSR models have introduced various techniques to enhance performance. VRT [30] enables parallel processing of long video sequences using a mutual attention mechanism for feature extraction, alignment, and fusion. RVRT [29] combines parallel and recurrent approaches, employing guided deformable attention for precise clip alignment. IART [54] uses implicit resampling with local cross-attention to preserve frequency details while reducing spatial distortions. DiQP [11], the first model for 8K videos, employs Denoising Diffusion to counteract compression artifacts while maintaining robustness across varying levels.

2.3. Federated Learning on Super Resolution Task

For low-level vision tasks, FedMRI [15] introduces a federated learning framework for MRI reconstruction with a shared encoder for generalized features and client-specific decoders for personalization. FedPR [16] improves image quality using pre-trained models and prompt learning with minimal trainable parameters. p²FedSR [55] enhances privacy-preserving SR by integrating client-specific degradation priors and a selective model aggregation strategy for personalized FL. FedSR [56] employs a detail-assisted contrastive loss for feature alignment at the client level and a hierarchical aggregation policy at the server level with historical global model, optimizing layer-wise model integration.

3. Preliminaries

3.1. VSR Problem Definition

VSR enhances video resolution by using multiple low-resolution frames, leveraging temporal information to exploit inter-frame dependencies, unlike SISR.

Problem Formulation In addition to the widely used RGB color space, other representations such as the YUV and YCbCr color spaces are frequently employed in VSR applications. Let $F_i \in \mathbb{R}^{H \times W \times 3}$ denote the i -th frame in a given LR video sequence, while $\hat{F}_i \in \mathbb{R}^{sH \times sW \times 3}$ represents its corresponding high-resolution (HR) counterpart, where s is the scaling factor (e.g., $s = 2, 4, 8$). Additionally, we define a set of $2N + 1$ HR frames $\{\hat{I}_j\}_{j=i-N}^{i+N}$ centered around \hat{I}_i , where N represents the temporal radius. The degradation process that generates an LR video sequence from its HR counterpart can be mathematically formulated

as:

$$I_i = \phi(\hat{I}_i, \{\hat{I}_j\}_{j=i-N}^{i+N}; \theta_\alpha) \quad (1)$$

where $\phi(\cdot; \cdot)$ is the degradation function parameterized by θ_α , incorporating various degradation factors such as noise, motion blur, and down-sampling effects.

A more detailed expression for the degradation process can be written as:

$$I_j = DBE_{i \rightarrow j}(\hat{I}_i) + n_j \quad (2)$$

where D represents the down-sampling operation, B denotes the blurring effect, $E_{i \rightarrow j}$ is a warping function that accounts for motion between frames \hat{I}_i and \hat{I}_j , and n_j represents the image noise. The goal of a VSR algorithm is to reconstruct an HR video sequence from degraded LR frames in a manner that closely resembles the ground truth video. This makes this task an ill-posed problem because there exist infinitely many possible HR images \hat{I}_i that can produce the same LR image I_i after degrading, meaning the degradation operator is highly non-injective [49]. While some of the techniques used in ISIR can be applied to individual frames, VSR must also consider inter-frame dependencies to ensure motion coherence across the sequence. The inverse process of degradation, which represents the super-resolution task, can be expressed as:

$$\tilde{I}_i = \phi^{-1}(I_i, \{I_j\}_{j=i-N}^{i+N}; \theta_\beta) \quad (3)$$

where \tilde{I}_i is the estimated HR frame corresponding to the ground truth \hat{I}_i , and θ_β represents the model parameters involved in the reconstruction process [33].

3.2. FL Problem Definition

FL enables multiple clients to train a shared model collaboratively without sharing raw data, enhancing privacy and reducing communication overhead through local computations and periodic model aggregation.

Problem Formulation FL aims to minimize the following objective function across participating clients:

$$\min_{\mathbf{w}} F(\mathbf{w}) = \sum_{k=1}^K p_k F_k(\mathbf{w}) \quad (4)$$

where:

- K is the total number of clients,
 - p_k is the relative weight of client k (typically based on its dataset size),
 - $F_k(\mathbf{w})$ is the local loss function for client k ,
 - \mathbf{w} represents the global model parameters.
- Each client updates the global model locally:

$$\mathbf{w}_k^{t+1} = \mathbf{w}^t - \eta \nabla F_k(\mathbf{w}^t) \quad (5)$$

where η is the learning rate. The updated models are aggregated by the central server using a weighted averaging scheme:

$$\mathbf{w}^{t+1} = \sum_{k=1}^K p_k \mathbf{w}_k^{t+1} \quad (6)$$

Not all clients participate equally in every training round due to data heterogeneity, resource constraints, network instability, or other limitations [59]. Client averaging based on their contributions stabilizes training, reduces variance, and improves generalization [6].

However, weighting clients solely by dataset size, as in traditional FedAvg[36], does not fully capture their impact on model performance [44]. A client’s importance extends beyond data quantity and is also influenced by the quality of its model updates and the loss it generates during training. Based on [46], we implement an approach where clients with lower loss are typically better trained and can be assigned higher weights during averaging. This ensures improved overall performance by leveraging the robustness properties analyzed in the paper. It is worth noting that some works instead prioritize clients with higher loss to increase fairness [26]. This approach, which contrasts with a focus on final performance, is more common in the context of personalized federated learning.

By incorporating loss-based importance into the aggregation process, federated learning can achieve more reliable and efficient training. This adaptive weighting ensures that client updates more accurately reflect their significance in improving the global model, leading to a more stable and equitable learning process [17].

4. Methodology

VSR remains a challenging problem due to its ill-posed nature. Severe degradations amplify artifacts, making it difficult to balance detail enhancement and noise suppression. To improve generalizability, diverse training data and large batch sizes are needed, but this significantly increases computational costs [8]. FL adds further complexity to VSR due to real-world constraints [14] and the nature of the task. In heterogeneous environments, differences in client data distributions lead to biased updates, poor generalization [5], and inefficient model merging. Gradient mismatches [53] and parameter inconsistencies slow convergence [10]. Most FL algorithms are designed for image classification which can be considered as a well-posed problem [18]. However, VSR is an ill-posed task, requiring a further fundamental assessment of existing methods to ensure effective adaptation. For instance, FedProx assumes a certain degree of similarity across client data distributions, but in real-world applications, these distributions can vary significantly. When this assumption fails, models experience drift, leading to inconsistent local updates and poor generalization [13]. Simi-

larly, SCAFFOLD assumes unbiased client updates, yet in large-scale deployments, heterogeneous data causes significant divergence, slowing convergence. Moreover, its need for additional state information per client makes it impractical for large-scale FL systems due to communication and storage constraints [10]. Meanwhile, Other methods such as FedDisco[58] and MOON rely on class label distributions or logits, making them inherently task-specific rather than generalizable. This work proposes a solution to enhance the overall objective of VSR models while improving aggregation to mitigate these challenges.

4.1. Enhancing Loss Function for Federated VSR

Selecting a proper loss function as objective for VSR model is crucial and determine the overall output’s performance [47, 50] and as depicted in Fig.1. It is evident that existing FL algorithms has problems in capturing and generating details in the output. Since we aim to avoid adding computational overhead to the client by using adversarial or perceptual loss, and because our objective is to keep the model untouched, ensuring *FedVSR* remains model-agnostic, we introduce an additional term to the overall loss of model improve performance.

4.1.1. DWT for High-Frequency Preservation

One common failure in training VSR models is producing overly smooth outputs, meaning the trained model fails to capture high-frequency information. As a result, details and textures are missing from the output. Since the models we used are among the top-performing ones in a centralized setting, this suggests that the failure to restore high-frequency details is specifically related to training under the FL paradigm. To alleviate this, we leverage the Discrete Wavelet Transform (DWT), which has proven effective in super-resolution tasks [20, 61].

DWT is a multi-resolution signal decomposition technique that represents a signal in terms of approximation and detail coefficients at different scales. For a 2D signal (such as an image or video frame), DWT decomposes the signal into sub-bands of different frequencies and orientations such as:

- Approximation Coefficients F_i^{LL} (low-pass filtered in both dimensions).
- Horizontal Detail Coefficients F_i^{LH} (high-pass in vertical, low-pass in horizontal).
- Vertical Detail Coefficients F_i^{HL} (low-pass in vertical, high-pass in horizontal).
- Diagonal Detail Coefficients F_i^{HH} (high-pass in both dimensions).

One of the simplest wavelets used in DWT is Haar wavelet, which consists of a step function. It is computationally efficient and commonly used in image and video processing tasks. In this method each frame’s pixel values

are convolved with:

- Low-pass filter $h = \frac{1}{\sqrt{2}}[1, 1]$ to extract approximation coefficients.
- High-pass filter $g = \frac{1}{\sqrt{2}}[1, -1]$ to extract detail coefficients.

This process is repeated independently for each frame in the sequence.

The coefficient in those four sub-bands are calculated as:

$$F_i^{LL} = (F_i * h^T) * h, \quad F_i^{LH} = (F_i * h^T) * g \quad (7)$$

$$F_i^{HL} = (F_i * g^T) * h, \quad F_i^{HH} = (F_i * g^T) * g \quad (8)$$

The low-frequency component F_i^{LL} , contains the content and color information of the input frame, while the three high-frequency sub-bands capture detailed information about global structures and textures [43]. Therefore, for our loss helper term, we consider only the high-frequency sub-bands and ignore the low-frequency ones.

The loss is then computed pixel-wise in each sub-band between the predicted \bar{F} and ground truth \hat{F} frame at time step i :

$$L_i^{LH} = \bar{F}_i^{LH} - \hat{F}_i^{LH} \quad (9)$$

$$L_i^{HL} = \bar{F}_i^{HL} - \hat{F}_i^{HL} \quad (10)$$

$$L_i^{HH} = \bar{F}_i^{HH} - \hat{F}_i^{HH} \quad (11)$$

Then with the Charbonnier loss [9] we calculate the helper term \mathcal{L}_{DWT} :

$$\mathcal{L}_{\text{HiFr}} = \sum_i \sum_{s \in \{LH, HL, HH\}} \sqrt{L_i^{s^2} + \epsilon^2} \quad (12)$$

Now, we define the overall loss for the model with two weighted terms, one for the generic VSR loss \mathcal{L}_{VSR} and one for the DWT-based high-frequency loss $\mathcal{L}_{\text{HiFr}}$ as follows:

$$\mathcal{L}_{\text{total}} = \lambda_{\text{VSR}} \mathcal{L}_{\text{VSR}} + \lambda_{\text{HiFr}} \mathcal{L}_{\text{HiFr}} \quad (13)$$

As our experiments demonstrate (see Section 5.3), the optimal weight values are unbounded, meaning they are not constrained by the relationship $\lambda_{\text{VSR}} = 1 - \lambda_{\text{HiFr}}$ and can be independently adjusted for better performance.

4.2. Loss-Aware Aggregation for Federated VSR

To further enhance the model’s performance, we employ a greedy aggregation approach with a decay rate, inspired by MKL-SGD [46]. MKL-SGD improves robustness by selecting samples with the lowest loss during training, thereby mitigating the impact of outliers. Similarly, in our method, clients accumulate their loss values throughout local training and compute an average loss based on the number of

training steps. When sending their updated model weights to the server, they also transmit this average loss. At the server, we perform inverse weighted averaging, where each client’s weight is computed as $I_i = \frac{1}{\mathcal{L}_i}$ and adjusted using an adaptive step: $I'_i = I_i^\alpha$ where α controls the strength of loss-based weighting. To regulate this process, we introduce a decay rate that gradually reduces the effect of loss-based weighting over time, following: $\alpha = \alpha^{1 - \frac{t}{T}}$ where t is the current round and T is the total number of rounds. This ensures that early training benefits from loss-based prioritization, while later rounds transition smoothly toward standard averaging, balancing robustness and generalization. The overall algorithm is summarized in Algorithm 1.

Algorithm 1 Our Method

Require: Number of communication rounds T , Number of clients N , Learning rate η , Adaptive step α , Decay rate γ

Ensure: Global model weights W_T

- 1: Server Initialization Initialize global model W_0
 - 2: **for** $t = 1, \dots, T$ **do**
 - 3: Server selects a subset of clients randomly $S_t \subseteq \{1, \dots, N\}$
 - 4: **for each** client $i \in S_t$ in parallel **do**
 - 5: Client updates local model:
 - 6: Retrieve latest global model W_t
 - 7: Perform local training for E epochs with learning rate η
 - 8: Compute Local Loss:
 - 9: Compute model-specific loss \mathcal{L}_{VSR}
 - 10: Compute \mathcal{L}_{DWT} loss \mathcal{L}_{DWT}
 - 11: Compute total loss

$$\mathcal{L} = \lambda_{\text{VSR}} \mathcal{L}_{\text{VSR}} + \lambda_{\text{HiFr}} \mathcal{L}_{\text{HiFr}}$$
 - 12: Client updates local model:

$$\mathbf{w}_i^{t+1} = \mathbf{w}_i^t - \eta \nabla F_i(\mathbf{w}_i^t)$$
 - 13: Return updated weights W_i and loss value \mathcal{L}_i to server
 - 14: **end for**
 - 15: Server Aggregation: (Performed at the Server)
 - 16: Compute inverse loss weighting $I_i = \frac{1}{\mathcal{L}_i}$
 - 17: Apply adaptive step $I'_i = I_i^\alpha$
 - 18: Normalize inverse loss weights $w_i = \frac{I'_i}{\sum_{j \in S_t} I'_j}$
 - 19: Compute weighted model update $W_i^{\text{scaled}} = w_i \cdot W_i$
 - 20: Aggregate global model $W_{t+1} = \sum_{i \in S_t} W_i^{\text{scaled}}$
 - 21: Apply Decay Rate to Adaptive Step $\alpha = \alpha^{1 - \frac{t}{T}}$
 - 22: **end for**
 - 23: **return** Global model W_T
-

5. Experiments

5.1. setup

Dataset: Following [29, 30, 54], one of the most commonly used datasets for training VSR is REDS [40]. It contains 240, 30, and 30 sequences for training, validation, and testing, respectively, with each sequence consisting of 100 frames at a resolution of 720×1280 . The corresponding low-resolution (LR) frames are generated through bicubic downsampling from the high-resolution (HR) images.

Model	Algorithm	Less Heterogeneous						More Heterogeneous					
		REDS[40]			Vid4[31]			REDS[40]			Vid4[31]		
		PSNR \uparrow	SSIM \uparrow	LPIPS \downarrow	PSNR \uparrow	SSIM \uparrow	LPIPS \downarrow	PSNR \uparrow	SSIM \uparrow	LPIPS \downarrow	PSNR \uparrow	SSIM \uparrow	LPIPS \downarrow
VRT [30]	FedAvg[36]	29.71	0.8522	0.1916	24.88	0.7680	0.2446	28.85	0.8282	0.2200	24.60	0.7516	0.2557
	FedProx[27]	28.82	0.8281	0.2133	24.18	0.7341	0.2668	28.64	0.8236	0.2222	24.10	0.7256	0.2713
	SCAFFOLD[21]	28.59	0.8181	0.2228	23.99	0.7182	0.2737	28.17	0.8074	0.2318	24.04	0.7208	0.2739
	<i>FedVSR</i> (Ours)	29.86	0.8562	0.1908	24.92	0.7682	0.2393	29.03	0.8339	0.2123	24.73	0.7584	0.2492
RVRT [29]	FedAvg[36]	31.30	0.8877	0.1536	25.96	0.8156	0.1974	29.89	0.8578	0.1867	25.67	0.8040	0.2065
	FedProx[27]	30.09	0.8618	0.1899	25.20	0.7775	0.2330	29.59	0.8526	0.1943	25.02	0.7730	0.2353
	SCAFFOLD[21]	29.63	0.7967	0.2101	24.79	0.7317	0.2407	26.71	0.7142	0.2590	23.08	0.6441	0.3018
	<i>FedVSR</i> (Ours)	31.54	0.8922	0.1455	26.05	0.8191	0.1889	30.90	0.8811	0.1576	25.90	0.8131	0.1910
IART [54]	FedAvg[36]	30.56	0.8729	0.1695	25.43	0.7949	0.2118	29.52	0.8493	0.1909	25.04	0.7774	0.2272
	FedProx[27]	29.65	0.8500	0.1683	24.72	0.7599	0.2307	29.30	0.8444	0.1958	24.42	0.7505	0.2293
	SCAFFOLD[21]	30.29	0.8678	0.1692	25.18	0.7857	0.2084	29.26	0.8413	0.1992	24.85	0.7690	0.2278
	<i>FedVSR</i> (Ours)	30.88	0.8812	0.1556	25.54	0.8012	0.1990	29.76	0.8536	0.1887	25.26	0.7850	0.2220

Table 1. PSNR (\uparrow), SSIM (\uparrow), and LPIPS (\downarrow) comparison of FL algorithms across different VSR models and datasets under varying levels of heterogeneity.

This dataset features a variety of natural and handmade objects, locations, and diverse content, making it heterogeneous in decentralized settings [40]. To further evaluate *FedVSR* and assess its robustness in more realistic, highly heterogeneous scenarios, we conducted additional experiments using Kinetics-400 [22], a dataset primarily used for human action recognition. It includes 400 action classes with 306,245 videos, each approximately 10 seconds long, sourced from unique YouTube videos. Since Kinetics-400 contains videos of varying resolutions, we selected only those with a 720×1280 resolution to ensure a fair comparison with REDS. From the 400 classes, we randomly chose 40, and for each class, selected six videos, extracting 100-frame clips to match REDS’ format. Kinetics-400 is particularly well-suited for testing *FedVSR* under more extreme heterogeneity because, unlike professionally filmed datasets, its videos often exhibit camera shake, lighting variations, shadows, and background clutter [22]. This makes it a challenging but realistic benchmark for assessing the model’s adaptability in diverse and less controlled environments. For consistency with our experimental setup, we refer to REDS as the “less heterogeneous” dataset and Kinetics-400 as the “more heterogeneous” dataset, given the increased variability in content, motion, and environmental conditions in the latter.

Implementation Details: To maintain our objective of developing a model-agnostic framework, we did not alter the official parameters of the baseline VSR models. Instead, we used their recommended settings for training. We created 40 clients, each assigned six videos in both experimental setups. In the more heterogeneous setup, each client received videos from a single class; for example, one client had only “archery” videos, while another had only “making pizza” videos. In contrast, in the less heterogeneous setup, the six videos were randomly assigned to each client.

We set the total number of global rounds to 100, with each client performing one local round (epoch) per global round. In each round, we randomly selected four clients to perform training. After completing their local training, these clients sent their updated weights to the server for aggregation. All experiments were conducted using bi-cubic (BI) degradation.

Baselines: For our baseline, we use a combination of FedAvg[36], FedProx[27], and SCAFFOLD[21] from the FL side, along with VRT[30], RVRT[29], and IART[54] from VSR. We selected these FL methods as they are widely accepted and frequently used to benchmark core algorithmic performance in recent literature. While newer approaches like MOON[24], FedDyn[1], FedDisco[57], FedLAW[28] exist, they rely on task-specific assumptions such as logits, class-wise statistics, or server-side data proxies that do not translate well to low-level, regression-based tasks like VSR. On the other hand, existing FL-SR models such as FedSR, p²FedSR, and FedMRI are not directly comparable to *FedVSR* for two key reasons. First, they are tightly coupled to a specific model architecture: they require dividing the model into predefined blocks (“shallow–deep–upsampler”), which limits flexibility and demands structural changes to existing SR models. Second, these methods are stateful meaning each client must store additional data across training rounds, such as degradation descriptors, deep feature extractors, or previous model weights. This leads to significantly higher storage, computation, and coordination overhead. In contrast, *FedVSR* is designed to be both model-agnostic and stateless, making it simpler, more lightweight, and easier to apply in diverse real-world scenarios.

Evaluation Metrics: The evaluation metrics used for the experiments are Peak Signal-to-Noise Ratio (PSNR) and

Structural Similarity Index (SSIM) and Learned Perceptual Image Patch Similarity (LPIPS).

Reproducibility: To ensure our experiments are reproducible, we fixed the random seed, which doesn’t affect client selection, model initialization, etc. We used four NVIDIA A6000 GPUs for training, with each model under a federated learning algorithm taking an average 46 hours to train. For the baselines alone, this consumed 36 days (2 experiments \times 9 models+algorithms \times 2 days per run).

5.2. Results and Comparison

Quantitative Results: As shown in Table 1, our proposed *FedVSR* algorithm consistently outperforms other federated learning (FL) algorithms across all tested models and datasets. On average, *FedVSR* surpasses existing FL methods by a margin of 0.61 dB in PSNR and 0.022 in SSIM and 0.022 in LPIPS in less heterogeneous settings, while in more heterogeneous settings, the margins are 0.66 dB in PSNR and 0.028 in SSIM and 0.019 in LPIPS, demonstrating its robustness under challenging conditions. Among the evaluated models, RVRT benefits the most from *FedVSR*, achieving the highest performance margin. In contrast, IART shows the lowest overall improvement but still maintains a competitive edge over the baseline FL methods.

The observed performance trends in our experiments align with existing findings on FedProx and SCAFFOLD, further validating our results. As shown in Fig.2, *FedVSR* consistently achieves superior PSNR values across different VSR models and datasets, outperforming FedAvg, FedProx, and SCAFFOLD, particularly in later training rounds. This aligns with prior research on FedProx, which highlights its failure to reach the stationary points of the global optimization objective, even under homogeneous data distributions. The study suggests that FedProx’s limiting points may remain far from the true minimizer of the global empirical risk [48], which could explain its suboptimal performance in our experiments. Although FedProx may still generalize well by aggregating local data effectively in certain conditions, its weaker convergence properties become apparent in more heterogeneous scenarios. We also observe that FedProx is highly sensitive to the μ value during training. The original paper suggests $\{0.001, 0.01, 0.1, 1\}$ as candidate values and finds that $\mu = 1$ performs better in most cases. However, we notice that for any μ greater than 0.001, the VSR model struggles significantly with learning. This suggests that the relationship is more complex and requires further investigation and analysis.

Similarly, our findings regarding SCAFFOLD’s inefficiency in highly heterogeneous settings corroborate previous research that highlights its susceptibility to instability under heterogeneous data [4]. The significant performance drops and stagnation observed in our experiments, particu-

larly with the RVRT model, align with the reported issues of SCAFFOLD transmitting nearly twice the data of other algorithms due to its reliance on control variates. This added communication burden does not necessarily translate to better convergence, as our results show that SCAFFOLD struggles to optimize effectively in diverse settings. Prior work [4] also notes that SCAFFOLD is highly prone to sudden performance breakdowns when gradient clipping is not employed, which is reflected in our results where its PSNR fluctuates or plateaus early in highly heterogeneous scenarios. The increased variance in SCAFFOLD’s performance under skewed data distributions further supports our findings that it fails to adapt smoothly across different client datasets, reinforcing its limitations in federated VSR tasks.

Overall, these existing studies provide strong theoretical support for our experimental results. In contrast, *FedVSR*’s convergence, stability, and robustness across varying levels of data heterogeneity highlight its effectiveness in overcoming these limitations.

Qualitative Results: As shown in Fig. 1 clearly demonstrate the limitations of FedAvg, FedProx, and SCAFFOLD in accurately reconstructing fine details. While these methods reduce some pixelation from the LQ input, they all fail to recover the textures and sharp edges present in the ground-truth. FedAvg produces overly smooth results, blurring important structural details such as the wooden lattice and frame edges. FedProx exhibits similar blurring, struggling to restore high-frequency textures. SCAFFOLD, not only fails to produce a sharp reconstruction but also introduces noticeable artifacts, distorting the texture of the wooden lattice and making the output appear unnatural. In contrast, *FedVSR* delivers significantly sharper and more realistic reconstructions, clearly outperforming the other approaches. Due to space limitations, additional qualitative and quantitative results are provided in the supplementary material 8.

5.3. Ablation Study

Evaluating $\mathcal{L}_{\text{HIFr}}$ Loss and Adaptive Aggregation To further analyze the impact of the DWT loss term and loss-aware adaptive aggregation, we conducted a series of experiments. Using FedAvg as a baseline, we added each component separately to evaluate their individual effects. To assess the impact of the $\mathcal{L}_{\text{HIFr}}$ term, we applied it to FedAvg and observed the changes ($F-\mathcal{L}_{\text{HIFr}}$). Similarly, to evaluate loss-aware adaptive aggregation, we first trained VSR models using a greedy aggregation strategy (F-GLA) that prioritizes low-loss updates in all rounds. We then compared this approach to an adaptive version that incorporates a decay mechanism (F-ALA). As shown in Table 2, the DWT loss term consistently outperforms loss-aware adaptive aggregation in all cases. Additionally, both methods individ-

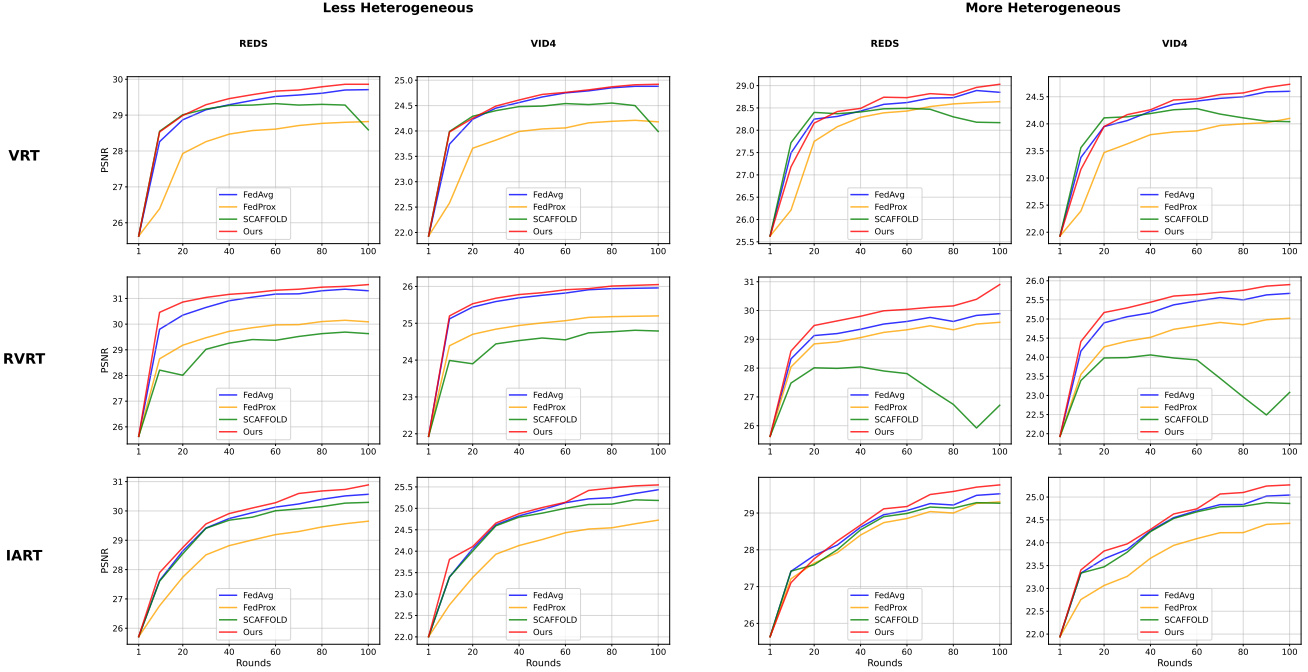


Figure 2. PSNR values across different rounds for various test sets under different settings for VRT [30], RVRT [29], and IART [54].

ually surpass FedAvg [36]. However, in some cases, the greedy aggregation strategy resulted in only marginal improvements or even a drop in overall performance especially in “more heterogeneous” setting based on PSNR and SSIM metrics. These findings further highlight the importance of high-frequency information not only for improving overall performance but also as a reliable metric for identifying valuable client weights. Due to space limitations, LPIPS metric results are provided in the supplementary material 7

both bounded and unbounded conditions. Due to the high computational cost of the experiments, we trained the VSR models for only 20 rounds and selected the best-performing configurations. Our results show that for VRT[30], the optimal values for both parameters are 1. For RVRT[29], the best values are 1 and 0.5, while for IART[54], the optimal values are 0.5 and 0.5, respectively.

Empirical Fisher for Estimating Weights Importance Inspired by [35], we explored estimating the importance of each weight in client models to enhance aggregation using Empirical Fisher (EF) Information. EF approximates the Fisher information matrix by leveraging gradients collected during backpropagation after training. While this method led to slight performance improvements, it proved computationally too expensive for clients, making it impractical for our setting. A more efficient variant of EF was introduced in [52]; however, as it is tailored for classification tasks, we leave its adaptation to VSR for future work.

Model	Setting	Less Heterogeneous				More Heterogeneous			
		REDS		Vid4		REDS		Vid4	
		PSNR	SSIM	PSNR	SSIM	PSNR	SSIM	PSNR	SSIM
VRT	F- $\mathcal{L}_{\text{HiFr}}$	29.80	0.8543	24.91	0.7681	28.98	0.8322	24.70	0.7577
	F-ALA	29.75	0.8531	24.89	0.7681	28.90	0.8313	24.64	0.7559
	F-GLA	29.70	0.8523	24.86	0.7670	28.83	0.8279	24.55	0.7500
RVRT	F- $\mathcal{L}_{\text{HiFr}}$	31.42	0.8888	26.02	0.8178	30.24	0.8617	25.84	0.8042
	F-ALA	31.38	0.8880	26.00	0.8171	30.19	0.8601	25.79	0.8041
	F-GLA	31.31	0.8879	25.95	0.8155	29.88	0.8576	25.60	0.8032
IART	F- $\mathcal{L}_{\text{HiFr}}$	30.79	0.8801	25.46	0.8001	29.64	0.8508	25.21	0.7837
	F-ALA	30.70	0.8789	25.44	0.7998	29.60	0.8500	25.18	0.7831
	F-GLA	30.57	0.8730	25.42	0.7951	29.50	0.8482	24.99	0.7761

Table 2. Ablation study on the impact of $\mathcal{L}_{\text{HiFr}}$ and adaptive aggregation on PSNR and SSIM under different heterogeneity settings.

Optimal λ_s Using a grid search, we explored different values for λ_{VSR} and λ_{HiFr} to determine the optimal ones. We varied each parameter from 1 to 0.1 in steps of 0.1 under

6. Conclusion

In this work, we introduced *FedVSR*, the first FL framework specifically designed for VSR, addressing privacy concerns while preserving high-quality performance. Unlike existing FL approaches that struggle with low-level vision tasks, our model-agnostic and stateless design ensures adaptability across various VSR architectures without prior model knowledge or historical weight storage.

By incorporating a lightweight loss term, we effectively guide local updates and enhance global aggregation, resulting in notable performance improvements over general FL baselines. Our method functions as a plug-and-play solution, and extensive experiments confirm its superiority over existing FL approaches, demonstrating its potential for real-world, privacy-sensitive applications. Furthermore, our study highlights key challenges in applying FL to low-level vision tasks, offering valuable insights for future research in this under-explored domain. As the first FL-based approach for VSR, this work establishes a strong baseline and provides a clear research path for future advancements. Despite promising results, a gap remains between FL-based VSR and centralized approaches. Future research could refine the aggregation strategy with a more intelligent, task-specific approach tailored for low-level vision. Additionally, our loss-guided optimization could be further enhanced to improve stability and better address existing challenges in FL-based VSR.

References

- [1] Durmus Alp Emre Acar, Yue Zhao, Ramon Matas Navarro, Matthew Mattina, Paul N. Whatmough, and Venkatesh Saligrama. Federated learning based on dynamic regularization, 2021. 6
- [2] Tariq Al Shoura, Ali Mollaahmadi Dehaghi, Reza Razavi, Behrouz Far, and Mohammad Moshirpour. Sepe dataset: 8k video sequences and images for analysis and development. In *Proceedings of the 14th ACM Multimedia Systems Conference*, page 463–468, New York, NY, USA, 2023. Association for Computing Machinery. 1
- [3] Mohammed Aledhari, Rehma Razzak, Reza M Parizi, and Fahad Saeed. Federated learning: A survey on enabling technologies, protocols, and applications. *IEEE Access*, 8: 140699–140725, 2020. 2
- [4] Gustav A. Baumgart, Jaemin Shin, Ali Payani, Myungjin Lee, and Ramana Rao Kompella. Not all federated learning algorithms are created equal: A performance evaluation study, 2024. 7
- [5] Debora Caldarola, Barbara Caputo, and Marco Ciccone. Improving generalization in federated learning by seeking flat minima. In *European Conference on Computer Vision*, pages 654–672. Springer, 2022. 4
- [6] Debora Caldarola, Barbara Caputo, and Marco Ciccone. Window-based model averaging improves generalization in heterogeneous federated learning. In *Proceedings of the IEEE/CVF International Conference on Computer Vision*, pages 2263–2271, 2023. 4
- [7] Di Chai, Leye Wang, Liu Yang, Junxue Zhang, Kai Chen, and Qiang Yang. A survey for federated learning evaluations: Goals and measures. *IEEE Transactions on Knowledge and Data Engineering*, 2024. 2
- [8] Kelvin CK Chan, Shangchen Zhou, Xiangyu Xu, and Chen Change Loy. Investigating tradeoffs in real-world video super-resolution. In *Proceedings of the IEEE/CVF Conference on Computer Vision and Pattern Recognition*, pages 5962–5971, 2022. 4
- [9] Pierre Charbonnier, Laure Blanc-Feraud, Gilles Aubert, and Michel Barlaud. Two deterministic half-quadratic regularization algorithms for computed imaging. In *Proceedings of 1st international conference on image processing*, pages 168–172. IEEE, 1994. 5
- [10] Michael Crawshaw, Yajie Bao, and Mingrui Liu. Federated learning with client subsampling, data heterogeneity, and unbounded smoothness: A new algorithm and lower bounds. *Advances in Neural Information Processing Systems*, 36:6467–6508, 2023. 4
- [11] Ali Mollaahmadi Dehaghi, Reza Razavi, and Mohammad Moshirpour. Reversing the damage: A qp-aware transformer-diffusion approach for 8k video restoration under codec compression. In *Proceedings of the Winter Conference on Applications of Computer Vision (WACV)*, pages 1258–1267, 2025. 1, 3
- [12] Amar B Deshmukh and N Usha Rani. Fractional-grey wolf optimizer-based kernel weighted regression model for multi-view face video super resolution. *International Journal of Machine Learning and Cybernetics*, 10:859–877, 2019. 1
- [13] Canh T Dinh, Tung T Vu, Nguyen H Tran, Minh N Dao, and Hongyu Zhang. A new look and convergence rate of federated multitask learning with laplacian regularization. *IEEE Transactions on Neural Networks and Learning Systems*, 2022. 4
- [14] Boyu Fan, Siyang Jiang, Xiang Su, Sasu Tarkoma, and Pan Hui. A survey on model-heterogeneous federated learning: Problems, methods, and prospects. In *2024 IEEE International Conference on Big Data (BigData)*, pages 7725–7734. IEEE, 2024. 4
- [15] Chun-Mei Feng, Yunlu Yan, Shanshan Wang, Yong Xu, Ling Shao, and Huazhu Fu. Specificity-preserving federated learning for mr image reconstruction. *IEEE Transactions on Medical Imaging*, 42(7):2010–2021, 2022. 3
- [16] Chun-Mei Feng, Bangjun Li, Xinxing Xu, Yong Liu, Huazhu Fu, and Wangmeng Zuo. Learning federated visual prompt in null space for mri reconstruction. In *Proceedings of the IEEE/CVF Conference on Computer Vision and Pattern Recognition*, pages 8064–8073, 2023. 3
- [17] Jack Goetz, Kshitiz Malik, Duc Bui, Seungwhan Moon, Honglei Liu, and Anuj Kumar. Active federated learning. *arXiv preprint arXiv:1909.12641*, 2019. 4
- [18] Eldad Haber and Lars Ruthotto. Stable architectures for deep neural networks. *Inverse Problems*, 34(1):014004, 2017. 4
- [19] Miao Hu, Zhenxiao Luo, Amirmohammad Pasdar, Young Choon Lee, Yipeng Zhou, and Di Wu. Edge-based video analytics: A survey. *arXiv preprint arXiv:2303.14329*, 2023. 1
- [20] Huaibo Huang, Ran He, Zhenan Sun, and Tieniu Tan. Wavelet-srnet: A wavelet-based cnn for multi-scale face super resolution. In *2017 IEEE International Conference on Computer Vision (ICCV)*, pages 1698–1706, 2017. 4
- [21] Sai Praneeth Karimireddy, Satyen Kale, Mehryar Mohri, Sashank Reddi, Sebastian Stich, and Ananda Theertha Suresh. Scaffold: Stochastic controlled averaging for federated learning. In *Proceedings of the IEEE/CVF Conference on Computer Vision and Pattern Recognition*, pages 8158–8168, 2020. 4

- ated learning. In *International conference on machine learning*, pages 5132–5143. PMLR, 2020. 1, 2, 6, 3, 4
- [22] Will Kay, Joao Carreira, Karen Simonyan, Brian Zhang, Chloe Hillier, Sudheendra Vijayanarasimhan, Fabio Viola, Tim Green, Trevor Back, Paul Natsev, Mustafa Suleyman, and Andrew Zisserman. The kinetics human action video dataset, 2017. 6
- [23] Jaehong Kim, Youngmok Jung, Hyunho Yeo, Juncheol Ye, and Dongsu Han. Neural-enhanced live streaming: Improving live video ingest via online learning. In *Proceedings of the Annual conference of the ACM Special Interest Group on Data Communication on the applications, technologies, architectures, and protocols for computer communication*, pages 107–125, 2020. 1
- [24] Qinbin Li, Bingsheng He, and Dawn Song. Model-contrastive federated learning. In *Proceedings of the IEEE/CVF Conference on Computer Vision and Pattern Recognition (CVPR)*, pages 10713–10722, 2021. 6
- [25] Qinbin Li, Bingsheng He, and Dawn Song. Model-contrastive federated learning. In *Proceedings of the IEEE/CVF conference on computer vision and pattern recognition*, pages 10713–10722, 2021. 2
- [26] Tian Li, Maziar Sanjabi, Ahmad Beirami, and Virginia Smith. Fair resource allocation in federated learning. *arXiv preprint arXiv:1905.10497*, 2019. 4
- [27] Tian Li, Anit Kumar Sahu, Manzil Zaheer, Maziar Sanjabi, Ameet Talwalkar, and Virginia Smith. Federated optimization in heterogeneous networks. *Proceedings of Machine learning and systems*, 2:429–450, 2020. 1, 2, 6, 3, 4
- [28] Zexi Li, Tao Lin, Xinyi Shang, and Chao Wu. Revisiting weighted aggregation in federated learning with neural networks. In *Proceedings of the 40th International Conference on Machine Learning*, pages 19767–19788. PMLR, 2023. 6
- [29] Jingyun Liang, Yuchen Fan, Xiaoyu Xiang, Rakesh Ranjan, Eddy Ilg, Simon Green, Jiezhong Cao, Kai Zhang, Radu Timofte, and Luc V Gool. Recurrent video restoration transformer with guided deformable attention. *Advances in Neural Information Processing Systems*, 35:378–393, 2022. 2, 3, 5, 6, 8, 1
- [30] Jingyun Liang, Jiezhong Cao, Yuchen Fan, Kai Zhang, Rakesh Ranjan, Yawei Li, Radu Timofte, and Luc Van Gool. Vrt: A video restoration transformer. *IEEE Transactions on Image Processing*, 2024. 3, 5, 6, 8, 1
- [31] Ce Liu and Deqing Sun. On bayesian adaptive video super resolution. *IEEE Transactions on Pattern Analysis and Machine Intelligence*, 36(2):346–360, 2014. 6
- [32] Chengxu Liu, Huan Yang, Jianlong Fu, and Xueming Qian. Learning trajectory-aware transformer for video super-resolution. In *Proceedings of the IEEE/CVF conference on computer vision and pattern recognition*, pages 5687–5696, 2022. 1
- [33] Hongying Liu, Zhubo Ruan, Peng Zhao, Chao Dong, Fanhua Shang, Yuanyuan Liu, Linlin Yang, and Radu Timofte. Video super-resolution based on deep learning: a comprehensive survey. *Artificial Intelligence Review*, 55(8):5981–6035, 2022. 3
- [34] Quande Liu, Cheng Chen, Jing Qin, Qi Dou, and Pheng-Ann Heng. Feddg: Federated domain generalization on medical image segmentation via episodic learning in continuous frequency space. In *Proceedings of the IEEE/CVF conference on computer vision and pattern recognition*, pages 1013–1023, 2021. 1
- [35] Michael S Matena and Colin A Raffel. Merging models with fisher-weighted averaging. *Advances in Neural Information Processing Systems*, 35:17703–17716, 2022. 8
- [36] Brendan McMahan, Eider Moore, Daniel Ramage, Seth Hampson, and Blaise Aguera y Arcas. Communication-efficient learning of deep networks from decentralized data. In *Artificial intelligence and statistics*, pages 1273–1282. PMLR, 2017. 1, 2, 4, 6, 8, 3
- [37] Jiaxu Miao, Zongxin Yang, Leilei Fan, and Yi Yang. Fedseg: Class-heterogeneous federated learning for semantic segmentation. In *Proceedings of the IEEE/CVF conference on computer vision and pattern recognition*, pages 8042–8052, 2023. 1
- [38] Crispian Morris, Nantheera Anantrasirichai, Fan Zhang, and David Bull. Dabit: Depth and blur informed transformer for joint refocusing and super-resolution. *arXiv preprint arXiv:2407.01230*, 2024. 1
- [39] Brian B Moser, Ahmed Anwar, Federico Raue, Stanislav Frolov, and Andreas Dengel. Federated learning for blind image super-resolution. *arXiv preprint arXiv:2404.17670*, 2024. 1
- [40] Seungjun Nah, Sungyong Baik, Seokil Hong, Gyeongsik Moon, Sanghyun Son, Radu Timofte, and Kyoung Mu Lee. Ntire 2019 challenge on video deblurring and super-resolution: Dataset and study. In *Proceedings of the IEEE/CVF Conference on Computer Vision and Pattern Recognition (CVPR) Workshops*, 2019. 2, 5, 6
- [41] Yifan Niu and Weihong Deng. Federated learning for face recognition with gradient correction. In *Proceedings of the AAAI conference on artificial intelligence*, pages 1999–2007, 2022. 1
- [42] Cheng Peng, Wei-An Lin, Haofu Liao, Rama Chellappa, and S Kevin Zhou. Saint: spatially aware interpolation network for medical slice synthesis. In *Proceedings of the IEEE/CVF Conference on Computer Vision and Pattern Recognition*, pages 7750–7759, 2020. 1
- [43] R Priyadharsini, T Sree Sharmila, and V Rajendran. A wavelet transform based contrast enhancement method for underwater acoustic images. *Multidimensional Systems and Signal Processing*, 29:1845–1859, 2018. 5
- [44] Pian Qi, Diletta Chiaro, Antonella Guzzo, Michele Ianni, Giancarlo Fortino, and Francesco Piccialli. Model aggregation techniques in federated learning: A comprehensive survey. *Future Generation Computer Systems*, 150:272–293, 2024. 4
- [45] M Dirk Robinson, Stephanie J Chiu, Cynthia A Toth, Joseph A Izatt, Joseph Y Lo, and Sina Farsiu. New applications of super-resolution in medical imaging. In *Super-resolution imaging*, pages 383–412. CRC Press, 2017. 1
- [46] Vatsal Shah, Xiaoxia Wu, and Sujay Sanghavi. Choosing the sample with lowest loss makes SGD robust. In *International Conference on Artificial Intelligence and Statistics*, pages 2120–2130. PMLR, 2020. 4, 5

- [47] Jie Song, Huawei Yi, Wenqian Xu, Xiaohui Li, Bo Li, and Yuanyuan Liu. Dual perceptual loss for single image super-resolution using esrgan. *arXiv preprint arXiv:2201.06383*, 2022. 4
- [48] Lili Su, Jiaming Xu, and Pengkun Yang. A non-parametric view of fedavg and fedprox: Beyond stationary points, 2022. 7
- [49] Dmitry Ulyanov, Andrea Vedaldi, and Victor Lempitsky. Deep image prior. In *Proceedings of the IEEE conference on computer vision and pattern recognition*, pages 9446–9454, 2018. 3
- [50] Subeesh Vasu, Nimisha Thekke Madam, and AN Rajagopalan. Analyzing perception-distortion tradeoff using enhanced perceptual super-resolution network. In *Proceedings of the European Conference on Computer Vision (ECCV) Workshops*, pages 0–0, 2018. 4
- [51] Jianyu Wang, Qinghua Liu, Hao Liang, Gauri Joshi, and H Vincent Poor. Tackling the objective inconsistency problem in heterogeneous federated optimization. *Advances in neural information processing systems*, 33:7611–7623, 2020. 1, 2
- [52] Xiaodong Wu, Wenyi Yu, Chao Zhang, and Phil Woodland. An improved empirical fisher approximation for natural gradient descent. In *The Thirty-eighth Annual Conference on Neural Information Processing Systems*, 2024. 8
- [53] Peng Xiao, Samuel Cheng, Vladimir Stankovic, and Dejan Vukobratovic. Averaging is probably not the optimum way of aggregating parameters in federated learning. *Entropy*, 22(3):314, 2020. 4
- [54] Kai Xu, Ziwei Yu, Xin Wang, Michael Bi Mi, and Angela Yao. Enhancing video super-resolution via implicit resampling-based alignment. In *Proceedings of the IEEE/CVF Conference on Computer Vision and Pattern Recognition*, pages 2546–2555, 2024. 3, 5, 6, 8, 1
- [55] Yue Yang and Liangjun Ke. Exploiting degradation prior for personalized federated learning in real-world image super-resolution. In *Proceedings of the 2024 International Conference on Multimedia Retrieval*, pages 146–154, 2024. 3
- [56] Yue Yang, Xiaodong Ren, and Liangjun Ke. Fedsr: Federated learning for image super-resolution via detail-assisted contrastive learning. *Knowledge-Based Systems*, 309:112778, 2025. 1, 3
- [57] Rui Ye, Mingkai Xu, Jianyu Wang, Chenxin Xu, Siheng Chen, and Yanfeng Wang. FedDisco: Federated learning with discrepancy-aware collaboration. In *Proceedings of the 40th International Conference on Machine Learning*, pages 39879–39902. PMLR, 2023. 6
- [58] Rui Ye, Mingkai Xu, Jianyu Wang, Chenxin Xu, Siheng Chen, and Yanfeng Wang. Feddisco: Federated learning with discrepancy-aware collaboration, 2023. 4
- [59] Yufeng Zhan, Jie Zhang, Zicong Hong, Leijie Wu, Peng Li, and Song Guo. A survey of incentive mechanism design for federated learning. *IEEE Transactions on Emerging Topics in Computing*, 10(2):1035–1044, 2021. 4
- [60] Xu Zhang and Jinxin Wu. Real-world video superresolution enhancement method based on the adaptive down-sampling model. *Scientific Reports*, 14(1):20636, 2024. 1
- [61] Chen Zhao, Weiling Cai, Chenyu Dong, and Chengwei Hu. Wavelet-based fourier information interaction with frequency diffusion adjustment for underwater image restoration. In *Proceedings of the IEEE/CVF Conference on Computer Vision and Pattern Recognition*, pages 8281–8291, 2024. 4
- [62] Joshua C Zhao, Saurabh Bagchi, Salman Avestimehr, Kevin S Chan, Somali Chaterji, Dimitris Dimitriadis, Jiacheng Li, Ninghui Li, Arash Nourian, and Holger R Roth. Federated learning privacy: Attacks, defenses, applications, and policy landscape-a survey. *arXiv preprint arXiv:2405.03636*, 2024. 2
- [63] Shangchen Zhou, Peiqing Yang, Jianyi Wang, Yihang Luo, and Chen Change Loy. Upscale-a-video: Temporal-consistent diffusion model for real-world video super-resolution. In *Proceedings of the IEEE/CVF Conference on Computer Vision and Pattern Recognition*, pages 2535–2545, 2024. 1

Supplementary Material

7. Extended Evaluation of HiFr Loss and Adaptive Aggregation Using LPIPS

To complement the analysis based on PSNR and SSIM discussed earlier in the paper, we present here an additional evaluation using LPIPS, which serves as a perceptual similarity metric. This acts as an extension to the previously discussed metrics and provides a more complete picture of model performance. Due to space limitations, we include this analysis here.

To evaluate the impact of the DWT loss term and the loss-aware adaptive aggregation strategies, we conducted a set of ablation experiments using FedAvg as the baseline. Each component was added independently to isolate its individual effect. Specifically, we assessed the contribution of the $\mathcal{L}_{\text{HiFr}}$ term by applying it to FedAvg (F- $\mathcal{L}_{\text{HiFr}}$), and examined two aggregation variants: a greedy loss-aware approach (F-GLA) that prioritizes updates from clients with lower losses, and an adaptive version (F-ALA) that incorporates a decay factor to regulate client influence over time.

As shown in Table 3 with LPIPS results, the observed trends remain largely consistent across metrics. The DWT loss term consistently provides more significant gains compared to the aggregation strategies, and both methods individually outperform the standard FedAvg baseline. However, similar to PSNR and SSIM, the greedy strategy sometimes leads to only marginal improvements or even minor performance degradation, especially under high heterogeneity. These findings underscore the importance of high-frequency information not only for boosting perceptual quality but also for reliably identifying valuable client updates.

Model	Setting	Less Heterogeneous						More Heterogeneous					
		REDS			Vid4			REDS			Vid4		
		PSNR	SSIM	LPIPS	PSNR	SSIM	LPIPS	PSNR	SSIM	LPIPS	PSNR	SSIM	LPIPS
VRT	F- $\mathcal{L}_{\text{HiFr}}$	29.80	0.8543	0.1910	24.91	0.7681	0.2399	28.98	0.8322	0.2130	24.70	0.7577	0.2500
	F-ALA	29.75	0.8531	0.1912	24.89	0.7681	0.2411	28.90	0.8313	0.2140	24.64	0.7559	0.2520
	F-GLA	29.70	0.8523	0.1914	24.86	0.7670	0.2436	28.83	0.8279	0.2198	24.55	0.7500	0.2555
RVRT	F- $\mathcal{L}_{\text{HiFr}}$	31.42	0.8888	0.1506	26.02	0.8178	0.1910	30.24	0.8617	0.1612	25.84	0.8042	0.1978
	F-ALA	31.38	0.8880	0.1518	26.00	0.8171	0.1931	30.19	0.8601	0.1728	25.79	0.8041	0.1992
	F-GLA	31.31	0.8879	0.1527	25.95	0.8155	0.1948	29.88	0.8576	0.1807	25.60	0.8032	0.2011
IART	F- $\mathcal{L}_{\text{HiFr}}$	30.79	0.8801	0.1588	25.46	0.8001	0.1999	29.64	0.8508	0.1899	25.21	0.7837	0.2231
	F-ALA	30.70	0.8789	0.1591	25.44	0.7998	0.2101	29.60	0.8500	0.1903	25.18	0.7831	0.2246
	F-GLA	30.57	0.8730	0.1690	25.42	0.7951	0.2119	29.50	0.8482	0.1929	24.99	0.7761	0.2284

Table 3. Ablation study on the impact of $\mathcal{L}_{\text{HiFr}}$ and adaptive aggregation on PSNR, SSIM, and predicted LPIPS under different heterogeneity settings.

8. Further Analysis: Performance Metrics and Visual Comparisons

This section provides additional performance evaluations for our proposed method. Figures 3, 5, and 7 illustrate the PSNR, SSIM and LPIPS trends across different rounds for multiple test sets under various configurations of VRT [30], RVRT [29], and IART [54]. These results further highlight the effectiveness of our approach in enhancing the performance across different models.

Figures 4, 6, and 8 provide qualitative visual comparisons on various test frames. Each figure presents a reference ground truth (GT) frame alongside low-quality (LQ) input and the outputs generated by different Federated Learning strategies, including FedAvg, FedProx, SCAFFOLD, and our method (FedVSR). The reconstructions show that FedVSR produces clearer and more visually faithful outputs, particularly in preserving finer details and reducing artifacts.

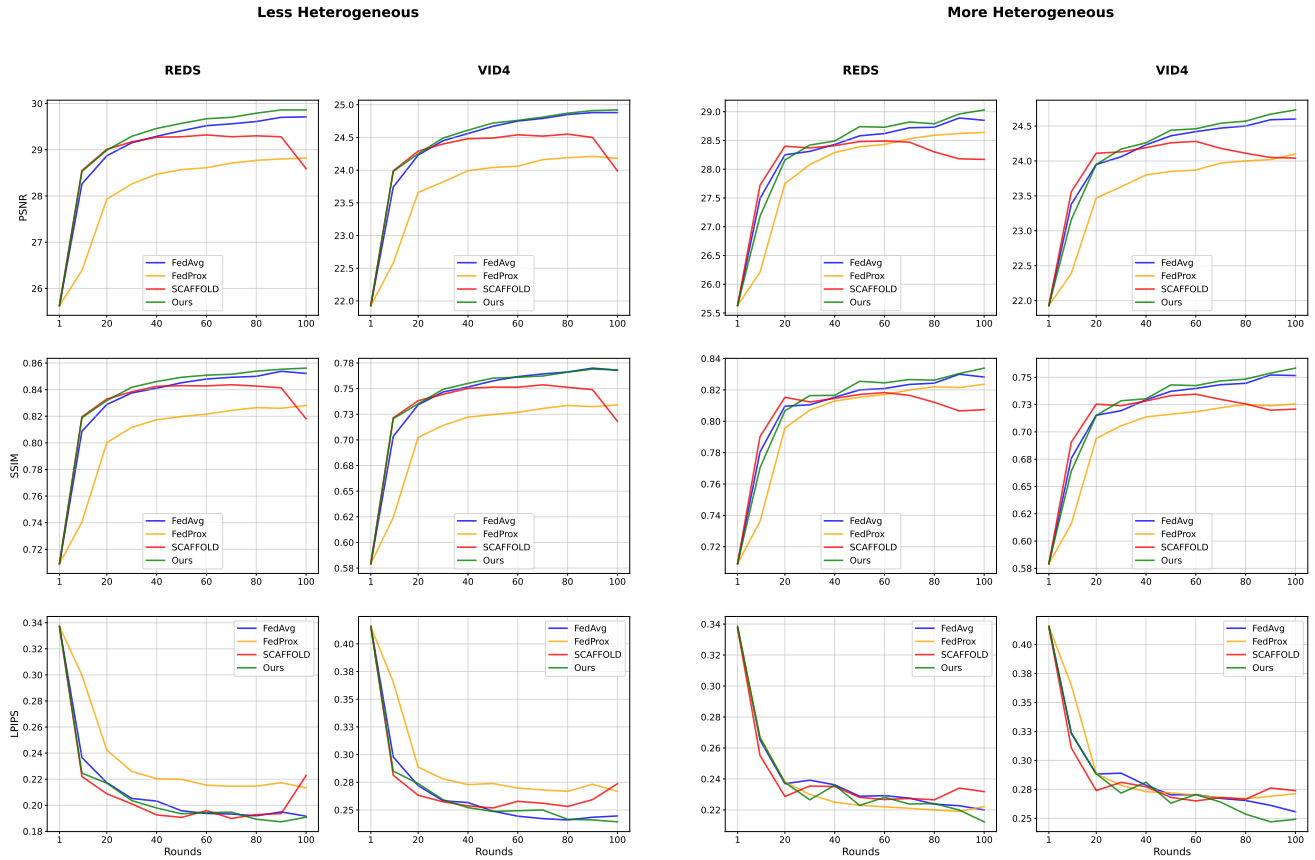


Figure 3. PSNR, SSIM and LPIPS values across different rounds for various test sets under different settings for VRT.

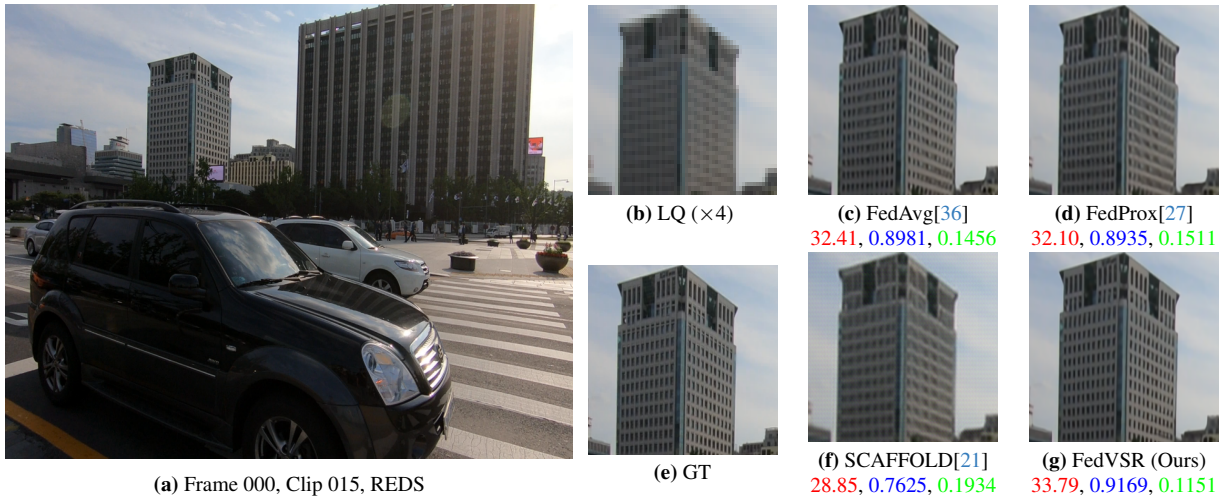


Figure 4. Comparison of RVRT output trained with different Federated Learning algorithms. PSNR, SSIM, and LPIPS metrics are shown in red, blue, and green respectively.

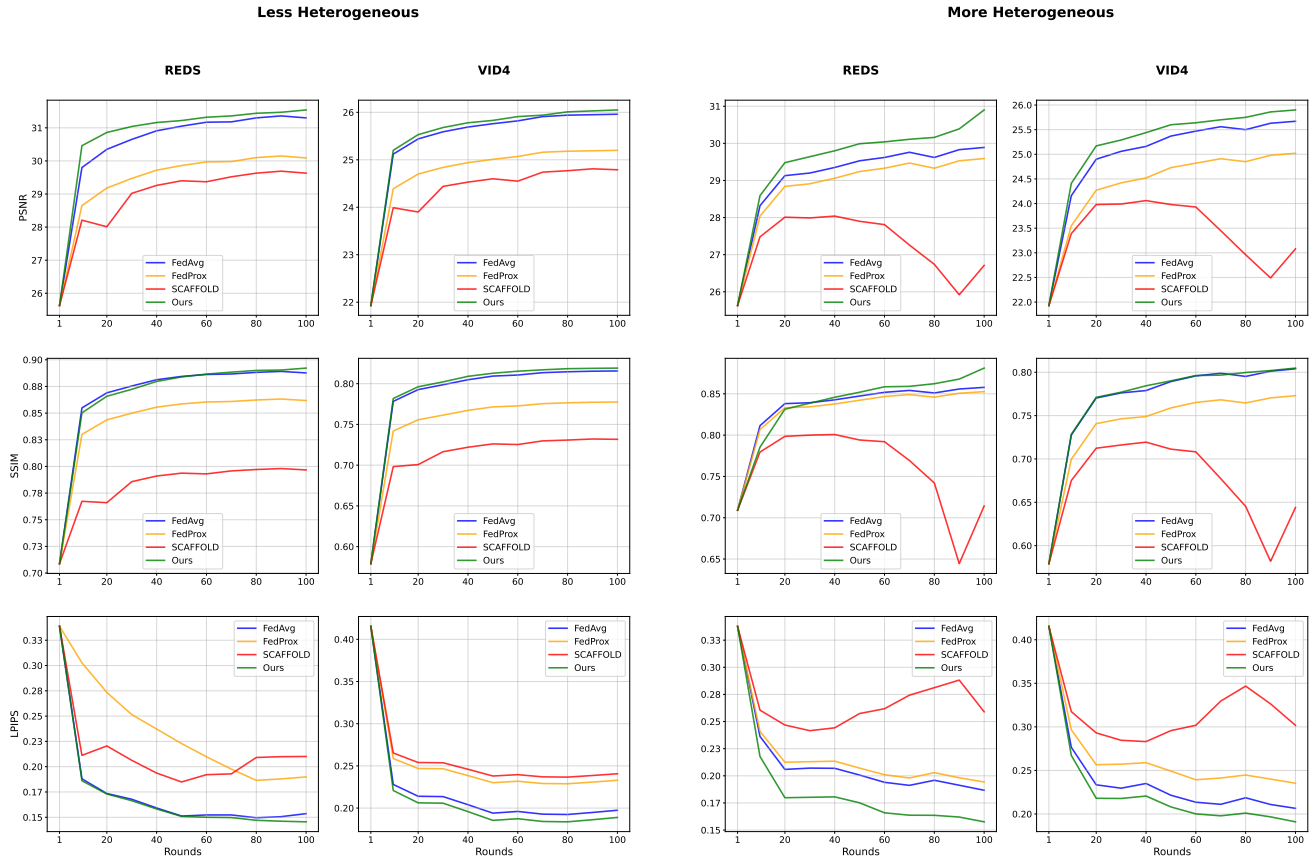


Figure 5. PSNR, SSIM and LPIPS values across different rounds for various test sets under different settings for RVRT.

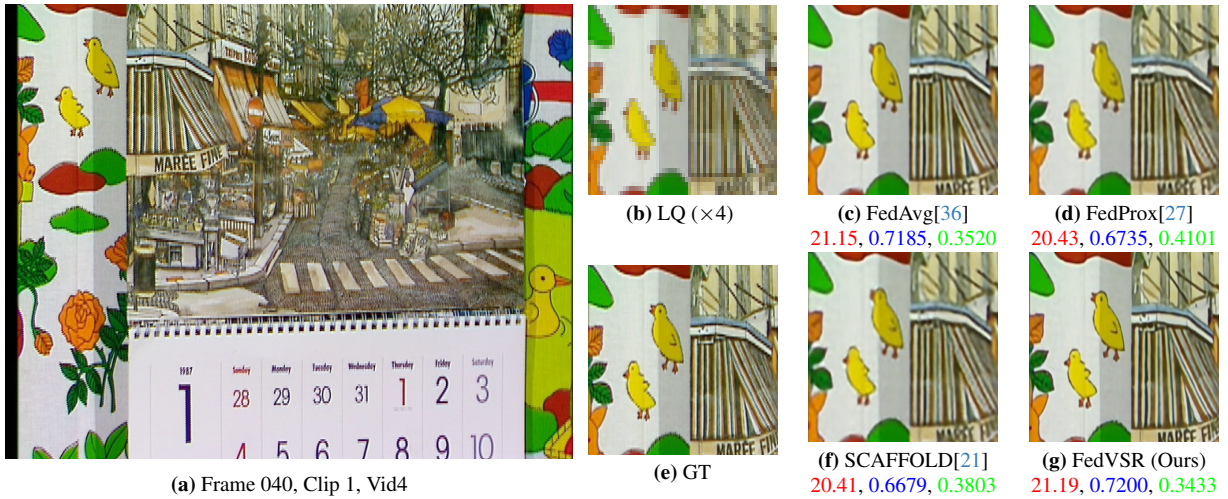


Figure 6. Comparison of VRT output trained with different Federated Learning algorithms. PSNR, SSIM, and LPIPS metrics are shown in red, blue, and green respectively.

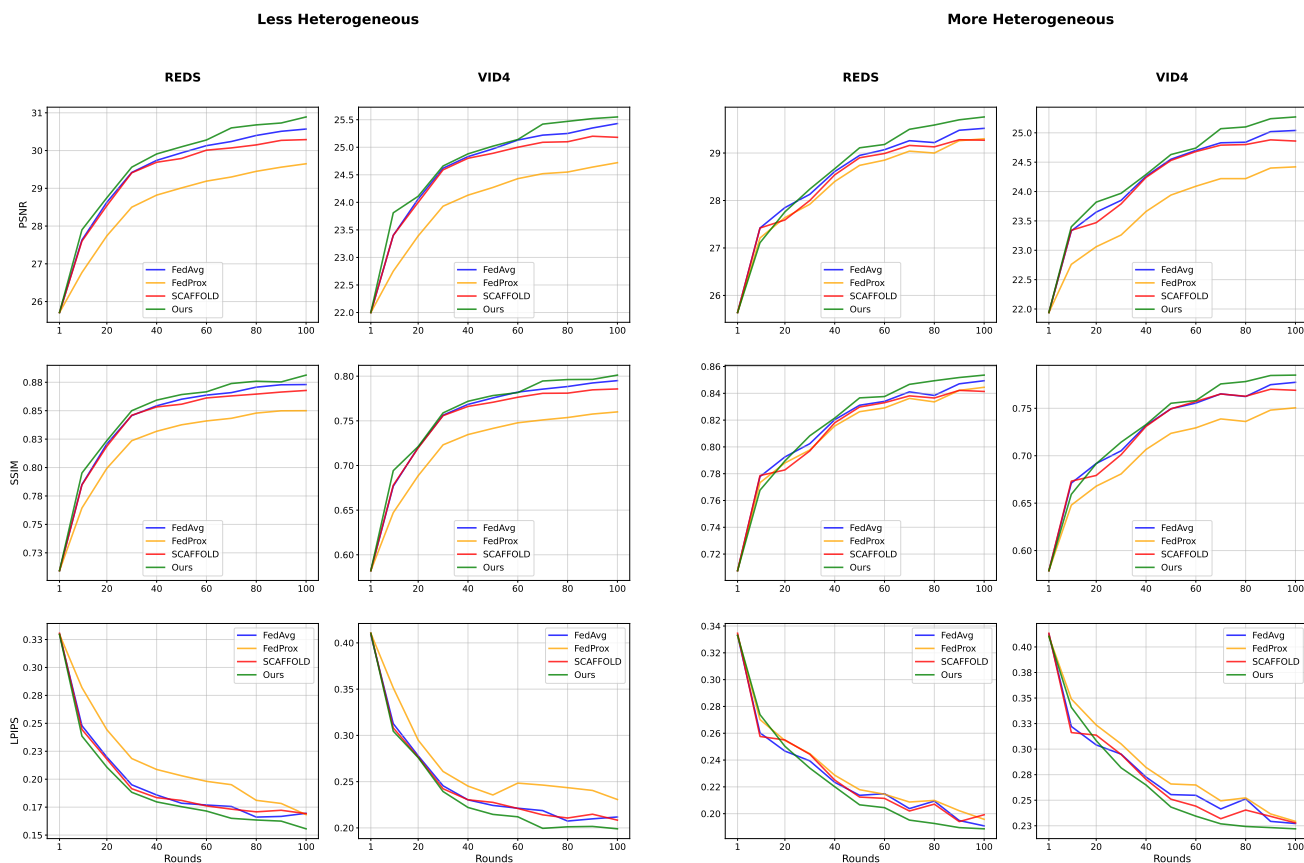


Figure 7. PSNR, SSIM and LPIPS values across different rounds for various test sets under different settings for IART.

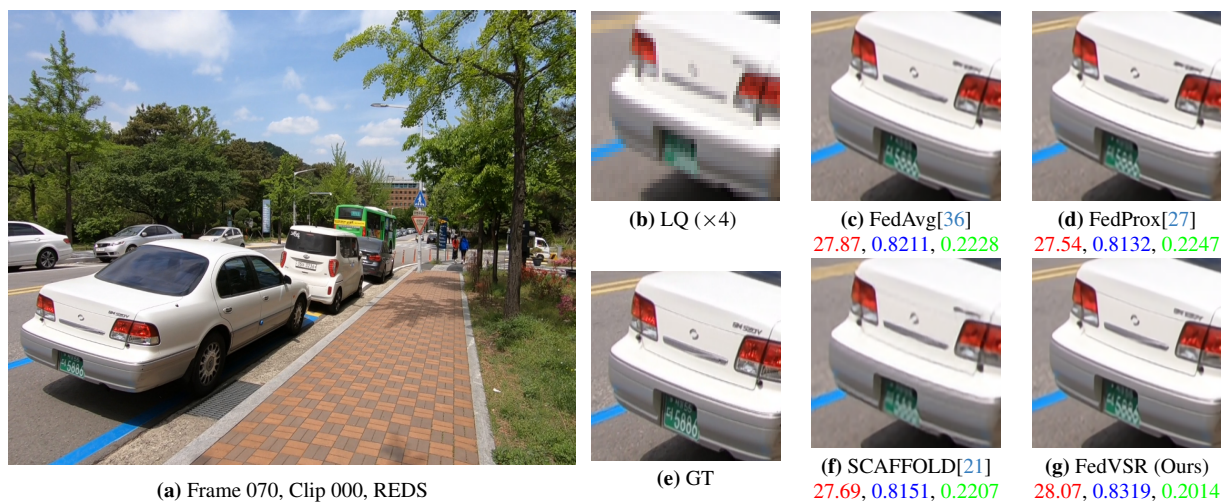


Figure 8. Comparison of IART output trained with different Federated Learning algorithms. PSNR, SSIM, and LPIPS metrics are shown in red, blue, and green respectively.